

# An Intelligent Control Strategy in a Parallel Hybrid Vehicle

Arezoo D. Abdollahi, S.K.Nikraves, M.B.Menhaj

Electrical Engineering, Department  
Amirkabir University of Technology, Tehran, Iran

## Abstract:

This paper presents a design procedure for an adaptive power management control strategy based on a driving cycle recognition algorithm. The design goal of the control strategy is to minimize fuel consumption and engine-out NO<sub>x</sub>, HC and CO emissions on a set of diversified driving schedules. Seven facility-specific drive cycles are considered to represent different driving scenarios. For each facility-specific drive cycle, the fuel economy and emission are optimized and obtained proper split between the two energy sources (engine and electric motor). A driving pattern recognition algorithm is subsequently developed and used to classify the current driving cycle into one of the facility-specific drive cycles; thus, the most appropriate control algorithm is adaptively selected. This control scheme was tested on a typical driving cycle and was found to operate satisfactorily.

**Keywords :** Hybrid vehicle, torque distribution, fuzzy rule base, neural network, drive cycle.

## 1. Introduction

A hybrid vehicle, using a combination of an internal combustion engine and electric motor, is an important concept to improve fuel economy and to reduce emission of vehicles as well. Therefore, Hybrid electric vehicles (HEVs) have great potential as new alternative means of transportation.

Design and implementation of HEVs present a number of challenging problems. The objective of the power management control strategy is to develop a near optimal power management strategy that determines the proper power split to minimize the fuel consumption and emissions of the hybrid vehicle. In addition, the control strategy also needs to ensure that the power demand from the driver is satisfied and the state of charge (SOC) in the battery is maintained within a pre-determined range under all driving conditions. The main challenge of the power

management problem arises from the complex and coupling nature of sub-system efficiencies, together with the diverse driving scenarios. In particular, management of energy and distribution of torque (power) are two of the key issues in the development of hybrid electric vehicles [1]-[5].

These issues can be summarized as follows:

1- How to meet the driver's torque demand while achieving both satisfactory fuel consumption and emissions.

2- How to maintain the battery state of charge (SOC) at a satisfactory level to enable effective delivery of torque to the vehicle over a wide range of driving situations.

In order to address these issues, an extensive set of studies has been conducted over the past two decades [1]-[16].

In particular, some logic based control strategies for distributing power demand have been suggested in Refs. [1]-[6]. These approaches are adopted mainly due to their effectiveness in dealing with problems appearing in the complexity of hybrid drive train via both heuristics (and human expertise) and mathematical models. However, these approaches generally do not address the driving situation that may affect the operation of the vehicle.

As noted in Refs. [7]-[9], the application of optimal control theory to power distribution for hybrid vehicles appears promising. In addition, a number of studies, dating back to 1980s, have focused on the application of dynamic programming to HEVs [10]-[11]. These and the aforementioned optimal control strategies are, however, generally based on a fixed drive cycle, and as such do not deal with the variability in the driving situation.

In view of this issue a number of alternative approaches have been proposed in the literature [12]-[13]. In particular, [14] formulated a drive cycle dependent optimization approach that selects the optimal power split ratio between the motor and the engine according to the characteristic features of the drive cycle.

With noting to their selective drive cycles that may not track any chosen pattern, the risk of misclassification may be high. Furthermore, they didn't mention anything about

initial condition at the start times of vehicle's driving, their results may be far from optimal results.

Another issue explained in [15],[16] is Intelligent Energy Management Agent (IEMA) that includes a driving situation identifier whose role is to identify the roadway type, the driving style of the driver as well as the current driving mode and trend. This information is subsequently integrated in a fuzzy logic based torque. Because of using the experimental results to generate fuzzy rules, there isn't any indicator to show how much it works optimally. Hence, the concept of fuel consumption and emission in hybrid vehicles is very sensitive to a drive cycle. So, if the driving control strategy of HEV is not suitable for a current drive cycle, vehicle performance can be worse than that of a conventional vehicle.

In this paper, there are three main topics. First, we develop an algorithm to cluster a current drive cycle as one of nine facility- specific drive cycles by using a neural network. Second, we introduce a control algorithm that adapts the driving control strategy to a current drive cycle using the driving cycle identifier. Third, if during the first 150s of driving, driving data is not sufficient to extract a rich set of driving information, we develop an algorithm to identify initial conditions.

In order to show the effectiveness of the proposed control strategy, we run some simulations. The results are promising. Finally, conclusions are drawn in the last part of the paper.

## 2. Selection of Seven Facility-Specific Drive Cycles

### 2.1. Facility-Specific Drive Cycles

we adopted a set of eleven drive cycles developed in Sierra Research Inc.[15],[17], each of which has its own facility-specific characteristics (for operation over a range of facilities on congestion levels, LOS<sup>1</sup>).

In [17], authors claimed the original area-wide cycle concept was to develop a family of composite driving cycles to represent overall travel within urban areas with different levels of congestion and average speed (facility-specific drive cycles).

We used these cycles to identify current drive cycle but some misclassification were occurred. So, we calculate their correlation to choose quasi-independent facility specific cycles. In order to do that, we should build characteristic parameters vector by using Table 2 (in section 2.2) for each facility-specific drive cycles and calculate their correlation (see Table 1).

**Table 1: The calculated correlation between facility specific drive cycles**

Drive Cycle	1	2	3	4	5	6	7	8	9	10	11
1	1	0.615	0.515	0.11	-0.15	-0.05	-0.025	-0.21	-0.1	-0.18	-0.38
2	0.615	1	0.61	0.04	0.02	0.07	0.004	0.33	0.40	0.53	0.42
3	0.515	0.61	1	0.12	-0.15	-0.01	0.005	-0.26	-0.16	-0.5	-0.40
4	0.11	0.04	0.12	1	0.7	0.2	0.22	0.37	0.15	0.015	-0.062
5	0.15	0.02	0.15	0.7	1	0.57	0.24	0.087	0.24	0.37	0.33
6	-0.05	-0.07	-0.01	0.2	0.57	1	0.021	-0.1	-0.11	0.25	0.29
7	0.025	0.004	0.005	0.22	0.24	0.021	1	0.14	0.19	0.059	0.0805
8	-0.21	-0.33	-0.26	0.37	0.087	-0.1	0.1	1	0.1	0.27	0.22
9	-0.1	-0.15	-0.16	0.15	0.15	-0.11	0.1	0.1	1	0.588	0.35
10	0.18	0.53	0.5	0.015	0.37	0.25	0.059	0.27	0.588	1	0.70
11	-0.38	-0.42	-0.40	-0.062	0.33	0.29	-0.0805	0.22	0.35	0.70	1

Regard to Table 1 , we can choose the drive cycles having correlation value more than "0.5" to be the same cycle. This threshold is selected in order to have enough drive cycles while they are quasi-independent. For example , cycle 2 can be considered as representative of cycles 1, 2, 3 and cycle 5 is representative of cycles 5 , 6 and cycle 11 is representative of 10 , 11. Furthermore we will use only seven facility specific cycles instead of eleven cycles (see Fig. 1.).

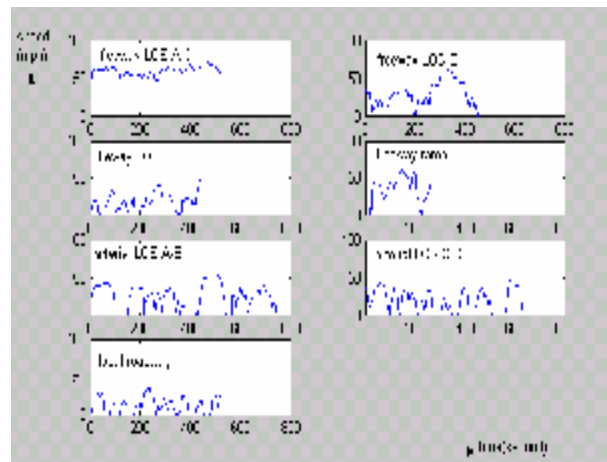


**Fig. 1: Facility-specific driving cycles**

### 2.2. Characteristic Parameters of a Drive Cycle

The mission of this part is to extract the key statistical features, or characteristic parameters of the driving pattern. While according to Ericsson [18] up 40 characteristic parameters may be extracted from a given drive cycle such as average speed, average acceleration and etc.(see Table 2).

<sup>1</sup> Level Of Service



**Table 2: Driving pattern parameters that were calculated for each driving cycle, v = speed , a = acceleration , r = deceleration ,Ericsson [18]**

Driving cycle parameter	
Average speed	% of time $2.5 > a > 1.5$ , $m/s^2$
Standard deviation of speed	% of time $1.5 > a > 1$ , $m/s^2$
Average acceleration	% of time $1 > a > 0.5$ , $m/s^2$
Acceleration Standard deviation	% of time $0.5 > a > 0$ , $m/s^2$
Average deceleration	% of time $0 > r > -0.5$ , $m/s^2$
Deceleration Standard deviation	% of time $-0.5 > r > -1$ , $m/s^2$
Number of adjacent max and min values of the speed curve $> 2km/h$ per 100s	% of time $-1 > r > -1.5$ , $m/s^2$
Number of adjacent max and min values of the speed curve $> 2km/h$ per 100m	% of time $-1.5 > r > -2.5$ , $m/s^2$
Number of adjacent max and min values of the speed curve $> 10km/h$ per 100s	% of time $r < -2.5$ , $m/s^2$
Number of adjacent max and min values of the speed curve $> 10km/h$ per 100m	% of time speed $< 2km/h$
Relative positive acceleration	Average stop duration
The integral of acceleration	Number of stops per kilometer
% of time $0 < v < 15$ , km/h	% of time when (v.a) $< 0$
% of time $15 < v < 30$ , km/h	% of time when (v.a) is 0-3
% of time $30 < v < 50$ , km/h	% of time when (v.a) is 3-6
% of time $50 < v < 70$ , km/h	% of time when (v.a) is 6-10
% of time $70 < v < 90$ , km/h	% of time when (v.a) is 10-15
% of time $90 < v < 110$ , km/h	% of time when (v.a) is $> 15$
% of time $v > 110$ , km/h	Average (v.a)
% of time $a > 2.5$ , $m/s^2$	Positive kinetic energy

### 2.3. A Neuro-based Drive Cycle Recognition

For real-time drive cycle recognition, we employ the Learning vector Quantization (LVQ) algorithm and its modifications [19]. For the purpose of classification, in this study a supervised competitive LVQ Network is

selected due to its effectiveness in the classification on complex and nonlinearly separable target classes [20].

#### 2.3.1. LVQ Network

A LVQ network classifies its input vector into one of the number of target classes through a two stage process. In the first stage, a competitive layer is used to identify the subclasses of input vectors. In the second stage, a linear layer is used to combine these subclasses into the appropriate target classes. The structure of the LVQ network is shown in Fig. 2.

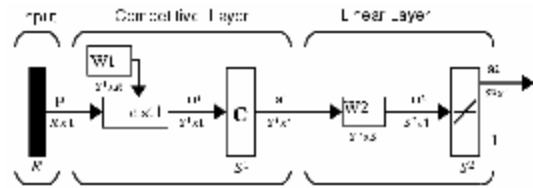


**Fig. 2: The LVQ network architecture**

Each neuron in the competitive layer of the network computes the Euclidean distance between the given input vector, p and a prototypical subclass vector w. With this in mind, for instance, the ith neuron in the competitive layer computes:

$$d = \|w_i - P\|$$

Subsequently, the competitive layer (designated as "C") assigns a 1 to the closest subclass to the given input vector and 0 to all other subclasses represented in the network. The linear layer combines the given identified subclasses into a (target) class.

#### 2.3.2. Training of LVQ Network and Validation

In order to train the LVQ network for roadway type classification, the statistics of nine facility-specific drive cycles (Fig. 1.) were calculated in terms of the characteristic parameters defined in Table 1. The initial training data set of the LVQ network is consisted of a  $[40 \times 7]$  matrix. When we validated this network, we figured out that five of 40 parameter in Table 2 have larger values in comparing with the others. They are:

- Average speed
- Max speed
- Trip time
- Relative positive acceleration

$$RPA = \frac{1}{x} \int va^+ dt, \quad x = \text{total distance,}$$

$$a^+ = \frac{dv}{dt} > 0, \quad v = \text{speed}$$

$$PKE : \frac{\sum (v_f^2 - v_s^2)}{x},$$

$$X = \text{distance, } V_f = \text{final speed, } V_s = \text{start speed}$$

Then, these parameters avoid other parameters to contribute in training. Thus following [15], each parameter value (input vector) was transformed into an array with entries of 1 and -1 as to four levels. For example, in case of first characteristic parameter (average speed), the value at each facility-specific drive cycles is 60.8, 29.84, 18.71, 34.29, 24.6, 19.12, 12.16 (mph) , so, their average  $m$  is 28.5(mph) and their standard deviation  $std$  is 16.04(mph). The level of each parameter is decided by three standards, which are  $m+a \times std$ ,  $m$ ,  $m-a \times std$  for example, if the value of any parameter is larger than  $m+a \times std$ , its level is 1, etc. (see Table 3).

**Table 3: Each parameter transforms into an array**

$P > m+a \times std$	Level 1: {1, 1, 1}
$m+a \times std > P > m$	Level 2: {1, 1, -1}
$m-a \times std < P < m$	Level 3: {1, -1, -1}
$P < m-a \times std$	Level 4: {-1, -1, -1}

$a$  is a tuning parameter and is chosen as 0.5. Because of this transformation, number of neurons in competitive layer is increased to avoid over training phenomenon.

We validated this network again and because of using single set of characteristic parameters for relatively long drive cycles [15], we still found indispensable error. Thus each drive cycle was divided into an appropriate number of 150 seconds that constitute subclasses of the whole drive cycle (its seven subclasses convert to approximately 33 subclasses).

In order to enhance the training performance of the network, we used LVQ 2.1 after LVQ for fine tuning of decision borders. (Kohonen [19] recommended that the learning process be started with LVQ, and if necessary continued by LVQ2.1, with a low initial learning rate value).

Learning here is similar to that in LVQ except two vectors of layer 1 that are closest to the input vector may be updated providing that one belongs to the correct class and one belongs to a wrong class and further providing that the input falls into a "window" near the mid plane of the two vectors.

The window is defined by [19]:

1. One of them should belong to the correct class (as the label of  $p$ ) and the other one to a wrong class.
2.  $p$  should fall in the window that is defined around the mid-plane of  $w_i$  and  $w_j$ . ( $p$  is defined to fall in the window

If

$$\frac{1-w}{1+w} < \frac{d_i}{d_j} < \frac{1+w}{1-w}$$

where  $d_i$  and  $d_j$  are the Euclidean distance of  $p$  from  $w_i$  and  $w_j$ , respectively. A relative window width  $W$  in the interval [0.2,0.3] is recommended by Kohonen, while its legitimate range is  $0 < W < 1$ .)

In the case of fulfilling the afore-mentioned conditions, the update rule is:

$$w_i(t+1) = w_i(t) + a(t)[p - w_i(t)]$$

$$w_j(t+1) = w_j(t) - a(t)[p - w_j(t)]$$

Let  $p$  be an input vector (from training set): where  $w_i$  is network weighting supposed to be in the same class as  $p$ , and  $w_j$  is network weighting in a different class.

Our competitive network give perfect match because we selected quasi-independent drive cycles in section 2.1 Then the results were verified with some test data which were obtained from ADVISOR's<sup>2</sup> default (for example, Fig. 4. and Fig. 14.) and actual drive cycles library with same Characteristic parameters. This LVQ network using the facility-specific driving cycle data given in [17], will be proper roadway type identifier (Fig. 3.).

Target =	class 1	class 2	class 3
	1 1 1 1 1	2 2 2 2	3 3
Network_output =	1 1 1 1 1	2 2 2 2	3 3
Target =	class 4	class 5	
	3 3	4 4 5 5 5 5 5 5 5	
Network_output =	3 3	4 4 5 5 5 5 5 5 5	
Target =	class 6	class 7	
	6 6 6 6 6 6	7 7 7 7 7	
Network_output =	6 6 6 6 6 6	7 7 7 7 7	

**Fig. 3: The result of network for classifying 7 drivecycles with considering 33 subclasses**

<sup>2</sup> ADvanced VehIcle SimulatOR



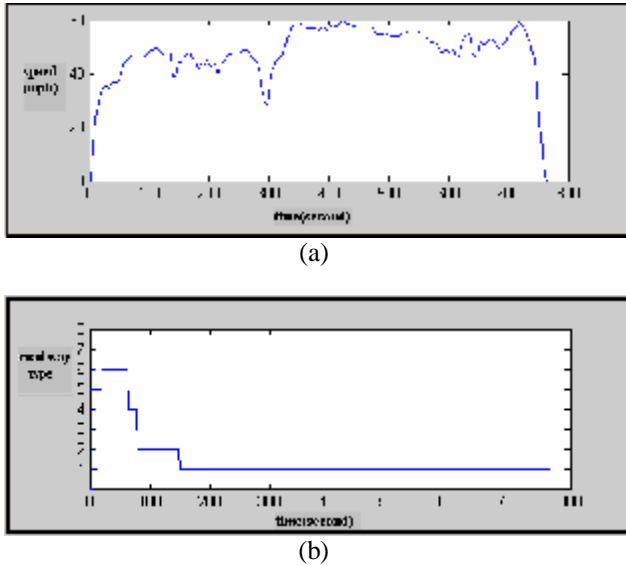


Fig. 4: (a) HWFET, One of the highway drive cycles of advisor's library. (b) Identified roadway type as will be explained in Table 4.

### 3. Control Strategy Implementation

#### 3.1. Optimization of Control Parameters at Each Facility-Specific Drivecycle

The control strategies' objective was minimum possible fuel consumption and emission for a given drive cycle. The behavior and the limitations of the powertrain's components were adapted by optimization process [13]. The method is an offline tool that is based on optimal control theory.

According to the mechanical arrangement, of the vehicle, (Fig.5.), the relationship between torques is [13]:

$$T_w = ((I_t(n_g)T_{ice} + I_b \cdot T_{em}) \cdot I_f \quad (1)$$

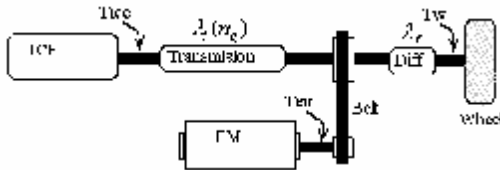


Fig. 5: Mechanical arrangement

Where  $T_w$  is the total torque required at wheel,  $T_{ice}$  is the torque provided by the ICE engine (positive only),  $T_{em}$  is the torque provided by the electric motor (positive or negative),  $I_t(n_g)$  is the gear ratio of the transmission and a function of the gear selected  $n_g$ ,  $I_b$  is the belt ratio of coupling between the electric motor and the drive

shaft and  $I_f$  is the gear ratio of final differential. Equation (1) above is a two degrees of freedom of three control variables  $T_{ice}$ ,  $T_{em}$  and  $n_g$ , because the value of  $T_w$  is defined at each time. The optimization process is performed under the mechanical constraints imposed by the driveline design [13].

$$\begin{aligned} 0 < T_{ice}(t) < T_{ice\_max} \\ T_{em\_min} < T_{em}(t) < T_{em\_max} \\ 0 \leq W_{em}(t) \leq W_{max} \\ W_{ice\_min} \leq W_{ice}(t) \leq W_{ice\_max} \end{aligned}$$

Where  $W_{ice}$  is speed of engine and  $W_{em}$  is speed of electric motor.

Another constraint is that the battery state of charge (SOC) is maintained within a prescribed range:

$$SOC_{low} < SOC(t) < SOC_{high}$$

Ideally the power distribution has to be chosen to minimize the overall engine fuel consumption over a given driving cycle within the constraints listed above, such as:

$$\text{Min} \sum_{\{T_{em}(t), n_g(t)\}} \dot{m}_f(t) \quad (2)$$

With  $\dot{m}_f(t)$  = Engine fuel flow rate.

In this study, regardless of dynamic model of vehicle, we consider a parallel HEV with static and quasi-static models in ADVISOR whose required power in driving is supplied by 41kw engine and 75kw electric motor. Thus, we have some efficiency map and lookup table for our optimization. Then, we used the approach which is based on static optimization methods.

We used equivalent fuel consumption  $\dot{m}_{feq}$  defined below instead of  $\dot{m}_f(t)$  (see (2)). Where the equivalent fuel flow rate cost function is simply defined as the sum of the actual fuel consumption of the engine and the equivalent fuel rate used due to the electric motor (positive or negative):

$$\dot{m}_{feq} = \dot{m}_f + \dot{m}_{fem}$$

Commonly, electric power is translated into an equivalent amount of (steady-state) fuel rate in order to calculate the overall fuel cost [22].

**Step 1:** Define the range of candidate operating points, represented by the range of acceptable motor torques for the current torque request [22]:

This relationship between engine, motor, and requested torque is described by (3). [22].

$$T_{engine} = T_{request} - \text{ratio} \times T_{motor} \quad (3)$$

Where:

ratio = motor-to-engine gear ratio

**Step 2:** For each candidate operating point, calculate the constituent factors for optimization [22 ]:

- Fuel energy consumed by engine:

For a given torque request and motor torque, Equation (3) sets the engine torque. At this torque and given speed, the engine map provides the fuel consumed by the engine (see Fig.6.).

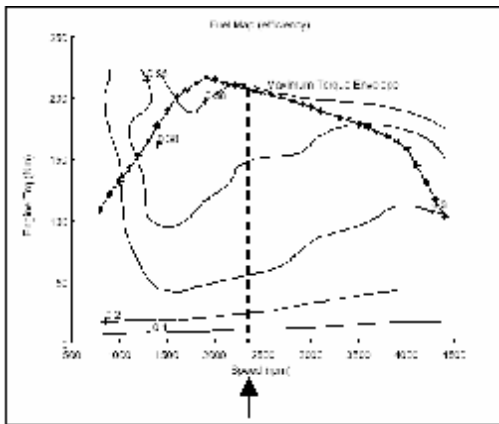


**Fig. 6: Engine energy efficiency map**

- Calculate the effective fuel energy that would be consumed by electromechanical energy conversion(equivalent):

Find fuel energy with respect to motor torque:

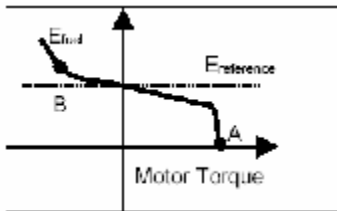


**Fig. 7: Fuel energy with respect to motor torque**

$E_{reference}$  in Fig. 7 indicates the case where  $T_{motor}$  is zero, or where engine supplies all of the requested torque. Find  $\Delta SOC$  with respect to motor torque,(see Fig. 8.).

In general, the relationship between  $\Delta SOC$  and motor torque is nonlinear for two reasons: 1) the motor efficiency map is nonlinear, and 2) charge and discharge resistances of batteries typically differ.

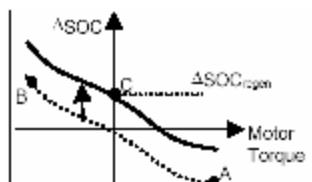


**Fig. 8:  $\Delta SOC$  with respect to motor torque**

During operation, a hybrid vehicle recaptures a certain amount of energy through regenerative braking. The

expected increase in SOC from regenerative braking is deemed “free energy” because no fuel energy must be consumed to obtain it.

Then, in order to apply a strategy at nine given drive cycles, we can run electric vehicle (the vehicle just have an electric motor) in ADVISOR and obtain  $\Delta SOC_{regen}$ , in battery when vehicle is in braking mode. Braking act in ADVISOR is distributed between driveline braking (regeneration) and friction braking (normal).

So, we first ran vehicle simulator (ADVISOR) at nine given drive cycles in electric mode (only there exists an electric motor in powertrain) when both of two kinds of braking (regeneration and friction) are considered. The second run included just friction braking. Difference between two obtained SOC results, would be  $\Delta SOC_{regen}$ .

To explain this procedure, we give an example. Consider a simple drive cycle with one braking part (as shown in Fig. 9. ). We obtain  $\Delta SOC_{regen}$  as mentioned above and it is shown in Fig.9 .

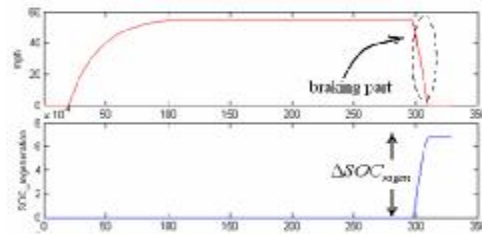


**Fig.9: a Drive cycle with its  $\Delta SOC_{regen}$**

Finally, combine the two curves given in figures 7,9 and into fuel energy as shown in Fig. 10.

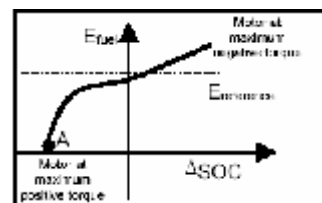


**Fig. 10.: Fuel energy with respect to motor torque**

- Emissions produced by engine:

The calculation of emissions produced over the range of torque is very similar to the engine energy consumption calculation (using emission maps).

**Step 3:** we first normalize each of them (energy and emission), then apply our weighting to their curves and finally compute the impact function (objective).

**Step 4:** Finally, we find minimum of the objective function and its corresponding torque.

This optimization scheme results in a proper split between the two energy sources using steady-state efficiency maps [13] , [21] . We carry out this optimization scheme at each facility-specific drive cycles and store engine torque ( $T_{engine}$ ), demand torque ( $T_{request}$ ) and state of charge (SOC) in each step.

### 3.2. Extracting Fuzzy Rule Base

After storing all data ( $T_{engine}$ ,  $T_{request}$ ,  $SOC$ ) calculated in the last part, we apply them to ANFIS toolbox in MATLAB ( $T_{request}$  &  $SOC$  as inputs and  $T_{engine}$  as an output) to extract a proper fuzzy rule base to implement the control strategy.(see Fig. 11. ).

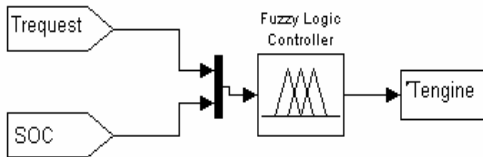


Fig. 11: Buzzy rule base controller

Then, we can find electric motor torque using (3).

### 3.3. Selection of Control Strategy in Current Driving Cycle

Fig.12. shows the concept of this control strategy, where “1 s” is the sampling time step for measuring vehicle input signals and generating control commands. First, characteristic parameters in the historical window ‘150 s’ are extracted, based on which the driving cycle over this historical window will be determined. Next, the control algorithm will be switched to the relative control algorithm corresponding to the newly identified facility-specific drive cycles. Finally, the control actions will continue for the next 5 seconds.

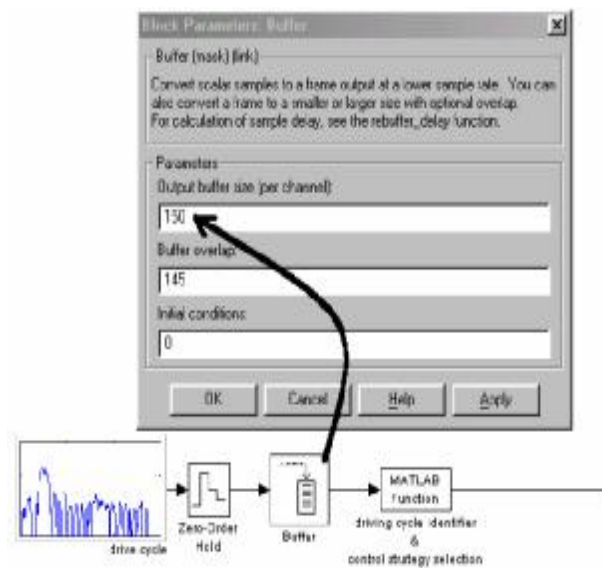


Fig. 12: Control strategy configuration

We run the program of characteristic parameter extraction and drive cycle recognition less than ‘0.71s’; we should notice that the sampling time step is 1 sec. Therefore, we may consider it as a real time procedure.

### 4. Identification of First 150s of Driving

Noting that during the first 150s of driving, driving data is not sufficient to extract a rich set of driving

information, so, we developed an algorithm to identify first 150s. We used a standard competitive network to identify initial conditions after starting the vehicle as we did in section 2. Although because of insufficient data we cannot extract all characteristic parameters that used in section 2, we only used 8 of them that were found to have large effects on either or all of emission factors of CO<sub>2</sub>, HC, and NO<sub>x</sub> (g/km) and fuel consumption (per 10 kilometers). Those were [18]:

- Factor for acceleration with strong power demand
- Stop factor
- Factor for acceleration with moderate power demand
- Extreme acceleration factors
- Factor for speed 50-70mph
- Factor for speed 70-90mph
- Deceleration factor
- Speed oscillation factor

We trained our network with these parameters and classified first seconds driving information as one of seven facility-specific drive cycles and switch to the corresponding control strategy.

Then we updated driving data each 5 seconds. So this competitive network give fairly good match and its result is better than that of random roadway type selection.

### 5. Simulation Results

In this section, we present the simulation study to evaluate the proposed energy management system. For the simulation study, a typical parallel drivetrain with manual 5-speed transmission is used. The models of the power train components are taken from [22]. The vehicle has a total mass of 1350 kg. An internal combustion engine with a displacement of 1.0 L, peak power of 41 kW and peak efficiency of 34% is chosen. In order to satisfy the requirement for acceleration, a motor with a power of 75 kW and peak efficiency of 92% is selected. The battery capacity of 26Ah (with 12v) with a weight of 275 kg is chosen. The battery’s type is VRLA. Typical parallel drivetrain is shown in Fig. 13.

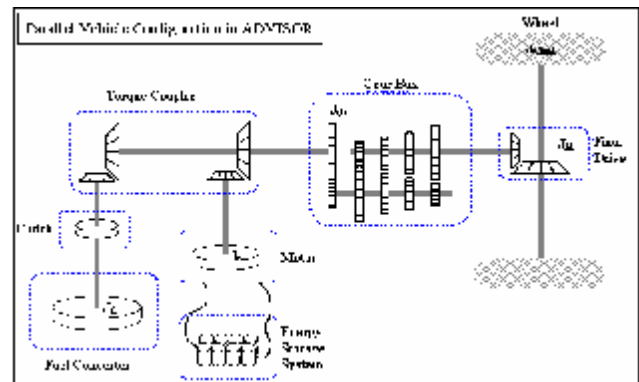
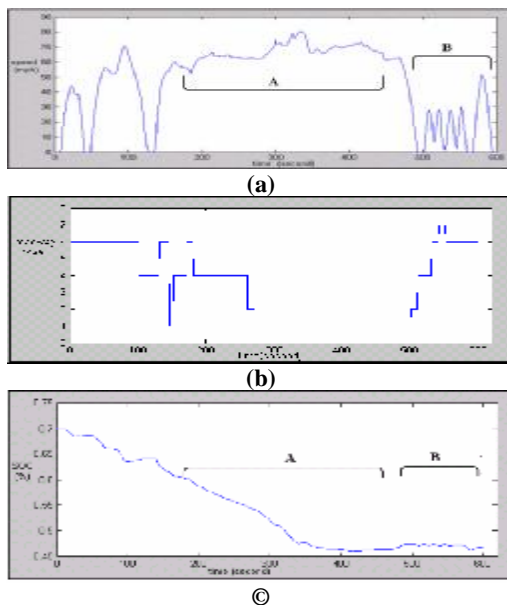


Fig. 13: Parallel hybrid vehicle configuration[22]

In this section, the performance of the vehicle under the supervision of our control strategy on the US06 is investigated. This drive cycle (US06) was developed to represent vehicle operation under urban driving conditions characterized as ones over a relatively long route that traverses numerous roadway links. The preliminary simulation study on the US06 indicates that the US06 (see Fig. 14.a ,14.b.) is a composite cycle that can be decomposed into different types of roadway. For instance, especially in this simulation, the US06 is decomposed into the facility-specific drive cycles considered (see Table 4) in this study as shown in Fig. 14.b .

**Table 4: Facility specific drive cycle**

Type	Facility specific drive cycle
1	Freeway under LOS A-C
2	Freeway under LOS E
3	Freeway under LOS F
4	Freeway ramp
5	Arterial under LOS A-B
6	Arterial under LOS C-D
7	Local roadway



**Fig. 14: (a) US06 drive cycle, (b) identified current drive cycle, (c) SOC varies in range 0.4 -0.7**

As shown in Fig. 14. a. and Fig. 14.c. two parts that marked A and B explain us some useful information. The drive cycle types identified in part A, belong to roadway types 1-4. So, in these road way types torque request will be high and we have too little regenerative SOC then SOC decrease fast. But in part B, current drive cycle belongs to roadway type 4-7. So, the torque request is

low and there exists sufficient amount of regenerative SOC that compensates the lack of battery's SOC.

We carried out the simulation in ADVISOR and compared our control strategy results with those of fuzzy logic control (baseline and emission mode [22]) in ADVISOR. The results show that our applied control strategy performance such as fuel-consumption and emission are superior, see Table 5.

**Table 5: Performance result on the US06**

US06	(mile/gal)	(grams/mile)		
	Fuel economy	HC	CO	NO <sub>x</sub>
Proposed control strategy	64.4	0.317	2.659	0.21
Emission mode	60	0.346	2.157	0.266
Baseline	35.4	0.536	7.977	0.508

## 6. Conclusions

A proposed control strategy based on the driving pattern recognition scheme was developed for a hybrid electric vehicle to minimize fuel consumption and engine-out emissions over various driving scenarios. So, we used seven facility-specific drive cycles developed in Sierra Research. And we developed a real-time driving cycle recognition algorithm using LVQ network. final algorithm was the control strategy which switches a current driving control strategy to the algorithm optimized in a recognized facility-specific drive cycle. then we verified the performance of this control strategy in fuel consumption and emission reduction by using an initial interval of driving identifier. The simulation results were very promising .

## Acknowledgment

The authors wish to thank professor Langari and Dr. Ericsson for their help.

## References

- [1] C. Liang, W. Qingnian, L. Youde, M. Zhimin, Z. Ziliang, and L. Di, "Study of the electric control strategy for the power train of hybrid electric vehicle", in Proc. of the IEEE International Vehicle Electronics Conf. (IVEC '99), vol. 1, Changchun, China, September 1999, pp. 383-386.
- [2] N. Jalil, N. A. Kheir, and M. Salman, "A rule-based energy management strategy for a series hybrid vehicle", in Proc. of the American Control Conf., vol. 1, Albuquerque, NM, June 1997, pp. 689 -693.
- [3] B. M. Brahma, "Intelligent control strategies for hybrid vehicles using neural network and fuzzy logic", Elect. Eng; ohio state univ. ,coluombos, 1997
- [4] N. J. Schouten, M. Salman, and N. Kheir, "Fuzzy logic control for parallel hybrid vehicles" ,IEEE Trans. on Cont.



Syst. Technology, vol. 10, no. 3, pp. 460-468, May 2002.

/advisor

[5] J.-S. Won and R. Langari, "Fuzzy torque distribution control for a parallel hybrid vehicle", *Expert Systems: The International Journal of Knowledge Engineering and Neural Networks*, vol. 19, no. 1, pp. 4-10, February 2002.

[6] M. Salman, N. J. Schouten, and N. A. Kheir, "Control strategies for parallel hybrid vehicles", in *Proc. of the American Control Conf.*, Chicago, IL, June 2000, pp. 524-528.

[7] A. Kleimaier and D. Schröder, "Optimization strategy for design and control of a hybrid vehicle", in *Proc.*, 6th International Workshop on Advanced Motion Control, Nagoya, Japan, March 30 - April 1 2000, pp. 459-464.

[8] S. Delprat, T. M. Guerra, and J. Rimaux, "Control strategies for hybrid vehicles: Optimal control", in *Proc.*, Vehicular Technology Conf. (VTC 2002-Fall), vol. 3, Vancouver, Canada, September 2002, pp. 1681-1685.

[9] S. E. Lyshevski and C. Yokomoto, "Control of hybrid-electric vehicles", in *Proc. of the American Control Conf.*, Philadelphia, PA, June 1998, pp. 2148-2149.

[10] A. Brahma, Y. Guezennec, and G. Rizzoni, "Optimal energy management in series hybrid electric vehicles", in *Proc. of the American Control Conf.*, Chicago, IL, June 2000, pp. 60-64.

[11] M. Oprean, V. Ionescu, N. Mocanu, S. Beloiu, and C. Stanciu, "Dynamic programming applied to hybrid vehicle control", in *Proc. of the International Conf. on Electric Drives (ICED 88)*, vol. 4, Poiana BRA W SOV, Romania, September 1988, pp. D2/10/1-20

[12] J.-S. Won, R. Langari, and M. Ehsani, "Energy management strategy for a parallel hybrid vehicle", in *Proc. of International Mechanical Engineering Congress and Exposition (IMECE '02)*, New Orleans, LA, November 2002, pp. IMECE2002-33460.

[13] G. Paganelli, M. Tateno, A. Brahma, G. Rizzoni, and Y. Guezennec, "Control development for a hybrid-electric sport-utility vehicle: Strategy, implementation and test results", in *Proc. of the American Control Conf.*, vol. 6, Arlington, VA, June 2001, pp. 5064-5069.

[14] C. C. Lin, S. Joen, H. Peng, J. M. Lee, "Driving pattern recognition for control of hybrid electric trucks"

[15] J.-S. Won and R. Langari, "Intelligent Energy Management Agent for a Parallel Hybrid Vehicle, Part I: System Architecture and Design of the Driving Situation Identification Process," *IEEE Transactions on Vehicular Technologies*, (accepted for publication 05/04.)

[16] J.-S. Won and R. Langari, "Intelligent Energy Management Agent for a Parallel Hybrid Vehicle, Part II: Torque Distribution and Charge Sustainment Strategies and Performance Results", *IEEE Transactions on Vehicular Technologies*. (accepted for publication 06/04.)

[17] T. R. Carlson and R. C. Austin, "Development of speed correction cycles", Sierra Research, Inc., Sacramento, CA, Report SR97-04-01, April 30 1997.

[18] E. Ericsson, "Independent driving pattern factors and their influence on fuel-use and exhaust emission factors", *Transportation Research Part D*, vol. 6, pp. 325-341. 2001.

[19] T. Kohonen, *Self-Organizing Map*, Springer, Berlin, 1995.

[20] M. B. Menhaj, "Computational Intelligence (vol.1), Fundamentals of neural networks", 2002

[21] C. Kim, E. NamGoong, and S. Lee, "Fuel Economy Optimization for Parallel Hybrid Vehicles with CVT", SAE Paper No. 1999-01-1148.

[22] ADVISOR 2002, NREL, [www.ctts.nrel.gov/analysis](http://www.ctts.nrel.gov/analysis)

